Single-Particle Motion and Heat Transfer in Fluidized Beds

Yee Sun Wong and Jonathan P. K. Seville
Centre for Formulation Engineering, Dept. of Chemical Engineering, University of Birmingham, Birmingham, B15 2TT, United Kingdom

DOI 10.1002/aic.11012
Published online October 31, 2006 in Wiley InterScience (www.interscience.wiley.com).

Fluidized beds are particularly favored as chemical reactors because of their ability to exchange heat through immersed heat-exchange surfaces. However, little is known about how the heat-exchange process works on a single-particle level. The most commonly applied theory of fluidized bed heat exchange is that developed by Mickley and Fairbanks in the 1950s—the so-called packet model. The work described in this article is an attempt to understand the process of heat transfer by solids convection, using positron emission particle tracking to follow the trajectory of a single tracer particle in the bed. In particular, the residence time of particles in the vicinity of the surface is determined here for the first time. Using these data, the observed heat-transfer variations are interpreted mechanistically. © 2006 American Institute of Chemical Engineers *AIChE J,* 52: 4099–4109, 2006

Keywords: fluidization, bed-to-surface heat transfer, horizontal tubes, positron emission particle tracking, packet model, particle residence time

Introduction

The main use of fluidized beds in the chemical industry is to carry out exothermic and endothermic reactions. In these cases, internal heat-transfer surfaces are usually introduced into the bed and these can enable good control of the bed temperature. However, the presence of internals may impair the solids movement in the bed, resulting in the variation of heat-transfer rate with position. The migration of particles to and from the heat-transfer surface is one of the determining factors of bed-to-surface heat transfer. Very early in the development of fluidized bed theory, Mickley and Fairbanks[1] developed the "packet renewal theory," which correlates the bed-to-surface heat transfer to the residence time of particles at the surface, although this theory is based on unverified assumptions. The present study makes a first attempt to interpret fluidized bed heat-transfer results using single-particle trajectories obtained by positron emission particle tracking (PEPT), a technique that allows the position of a single-particle tracer to be found very rapidly (about 100 s^{-1}) in three-dimensional (3D) movement. A detailed description of the technique can be found elsewhere.[2,3]

Bed-to-Surface Heat Transfer in Fluidized Beds

There are three physical mechanisms that contribute to the bed-to-surface heat-transfer process[4]: particle convection, interphase gas convection, and radiation. The last of these is of practical importance only at very high temperatures ($\gtrsim$800 K). For fine particles such as those of interest in most catalytic reactors, the particle convective component dominates, and this is the subject of the present work. Bed-to-surface heat transfer is limited by the thickness of the gas film between the surface and adjacent particles because most heat transfer occurs through a gas film around the contact points; this applies to both particle–particle and particle–surface heat transfer. With increasing particle diameter, the film thickness is increasingly limiting so that the importance of the interphase gas convective component then increases. The two extreme cases (where par-

Current address of Y. S. Wong: KBC Advanced Technology, 435 Orchard Road #16-02/03, Wisma Atria, Singapore 238877.
Correspondence concerning this article should be addressed to Y. S. Wong at ywong@kbcat.com.

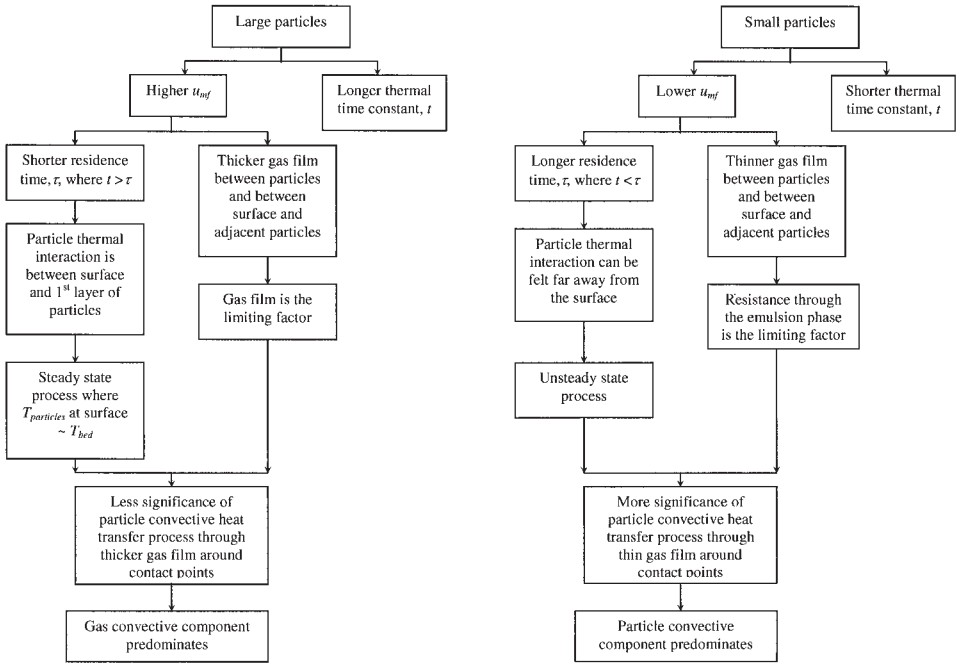

Figure 1. Bed-to-surface heat-transfer mechanisms for large and small particles.[6]

ticle convection and gas convection are controlling) will be discussed in detail later.

Gloski et al.[5] suggested consideration of the heat-transfer process in terms of the thermal time constant that characterizes the time for temperature change of a particle in contact with a surface. This time constant can be estimated as follows with the assumption that there is no temperature gradient within the particle itself:

$$t \sim \frac{1}{36}\frac{\rho_p C_p d_p^2}{k_g} \tag{1}$$

where ρ_p is the particle density (kg/m^3), C_p is the specific heat of the particle (J kg^{-1} K^{-1}), d_p is the particle diameter (m), and k_g is the thermal conductivity of the gas (W m^{-1} K^{-1}). In the case of larger particles (such as Group D particles), where the thermal time constant is much greater than the particle replacement time, the thermal interaction is limited to the region between the surface and the first layer of particles only. For this reason, the time-averaged heat-transfer coefficient is independent of the particle replacement frequency, given that the temperature of particles adjacent to the surface remains close to the bed temperature during the particle residence time. On the other hand, if the particle residence time is greater than the thermal time constant, the thermal properties of the dense "phase" will take control of the bed-to-surface heat transfer. This is the typical situation for smaller particles (for example, in Geldart's Group A).

The particle convective component is significantly dependent on the bed bubbling behavior and, in the range where heat transfer depends on particle renewal frequency, more vigorous bubbling is an advantage, at least in principle. However, at a high fluidizing velocity under conditions where the gas convective component is dominant, bed-to-surface heat transfer may be reduced, as the number of bubbles at the tube surface increases, resulting in a reduction of time-averaged solids concentration near the surface ("blanketing"). Because of the thermal time constant effect discussed above, however, the effect of increasing gas velocity on heat-transfer coefficient is different for different sizes of particles: for small particles, heat transfer depends on the particle replacement time, whereas for large particles, heat transfer is relatively independent of the particle residence time and is thus almost independent of gas

Table 1. Parameters for Eqs. 2 and 4

Effective thermal conductivity of homogeneous gas–solids medium[13,14]

Fixed bed with stagnant gas:

$$k_e^\circ = \varepsilon_{mf} k_g + \frac{(1-\varepsilon_{mf})k_s}{\phi_b\left(\frac{k_s}{k_g}\right) + \frac{2}{3}} \tag{5}$$

Between wall and fixed bed with stagnant gas:

$$k_{ew}^\circ = \varepsilon_w k_g + \frac{(1-\varepsilon_w)k_s}{\phi_w\left(\frac{k_s}{k_g}\right) + \frac{2}{3}} \tag{6}$$

Voidage near the wall region[15]

$$\varepsilon_w = 1 - \frac{(1-\varepsilon_{mf})[0.7293 + 0.5139(d_p/d_t)]}{1 + (d_p/d_t)} \tag{7}$$

Thermal resistance[9]

Thermal contact resistance at the wall:

$$R_w = \frac{d_p}{2k_{ew}^\circ} \tag{8}$$

Thermal resistance of packets of emulsion particles:

$$R_{packet} = \frac{1}{1.13}\left[\frac{\tau}{k_e^\circ \rho_p (1-\varepsilon_{mf}) C_p}\right]^{1/2} \tag{9}$$

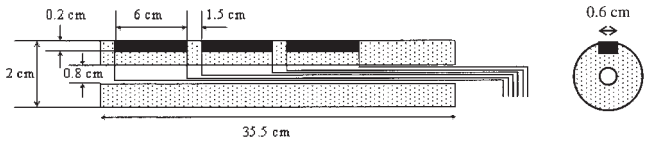

Figure 2. Heat-transfer probe.

velocity. Bed-to-surface heat transfer for these two extreme cases is summarized in Figure 1.

Mickley and Fairbanks[1] were the first to develop a model accounting for the role played by the particle heat capacity. This model is called the *packet renewal model*, which considers the bed-to-surface heat transfer as a transient renewal process. The heat resistance in this model is caused by a relatively thick dense phase layer. Based on the assumption that the heat-transfer process is controlled by unsteady-state conduction from (or to) the surface to (or from) a packet, the expression for the time-averaged heat-transfer coefficient for the dense phase packet is as follows:

$$h_{packet} = 1.13\left[\frac{k_e^{\circ}\rho_p(1-\varepsilon_{mf})C_p}{\tau}\right]^{1/2} \tag{2}$$

where k_e° is the effective thermal conductivity of the homogeneous gas-particle medium (W m^{-1} K^{-1}) and τ is the particle replacement time (s). The density and heat capacity of the packet are assumed to be those of the quiescent bed. As explained earlier, there is a limitation to this unsteady-state model when dealing with larger particles, where the bed-to-surface heat transfer becomes a nearly steady state process.[7]

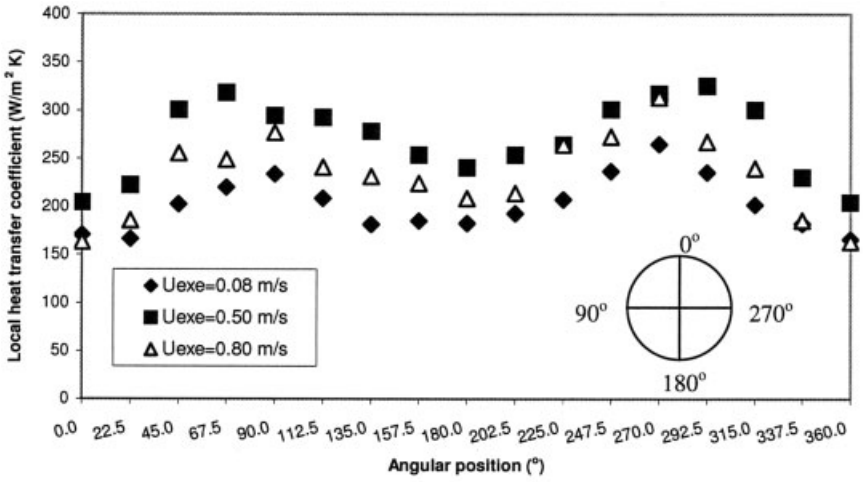

(a)

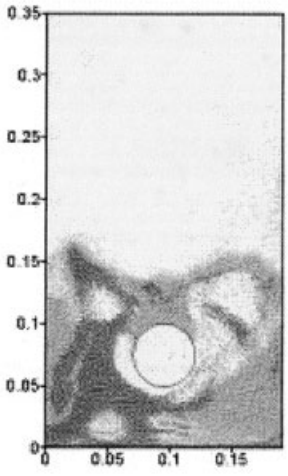

(b)

Figure 3. (a) Variation in local heat-transfer coefficient over the tube surface with excess gas velocity: cylindrical bed (ϕ 240 mm), 0.6 mm sand, bed static height 350 mm, and probe positioned with its axis 150 mm above the distributor; (b) DEM simulation of fluidized bed containing a single horizontal tube, showing "cap" of defluidized solids above the tube and gas pocket below.[6]

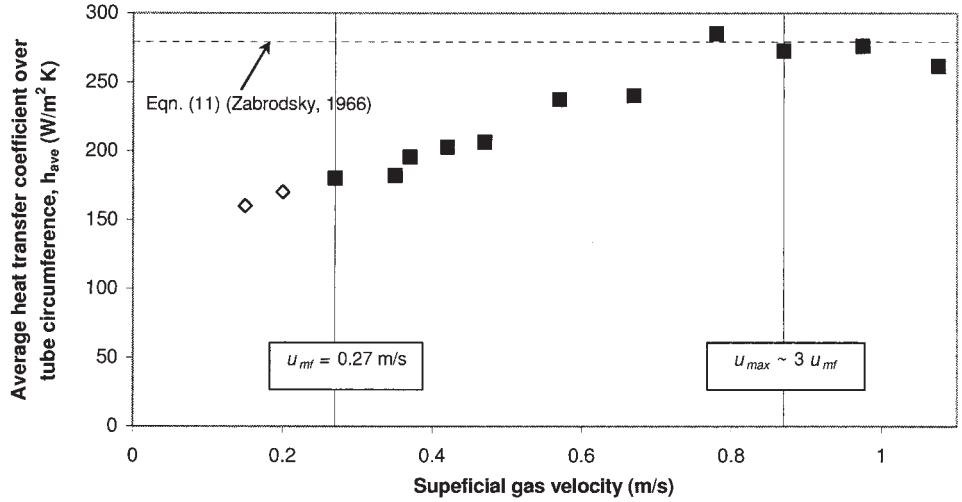

Figure 4. Dependency of average heat-transfer coefficient over the tube circumference on superficial gas velocity.

Cylindrical bed (ϕ 240 mm), 0.6 mm sand, bed static height 350 mm, and probe positioned at a bed level of 150 mm.

Ozkaynak and Chen[8] investigated the validity of the packet model for both large and small particles. From their experimental results, it was found that the packet model overpredicted the heat-transfer coefficient for large particles, whereas the model satisfactorily fitted small particles with different physical and thermal properties.

Gelperin and Einstein[9] derived a number of theoretical expressions for calculating both instantaneous and mean heat-transfer coefficients, which consider the presence of an effective gap between the particles and the surface, with different boundary conditions. A simple approximation for the case where the surface temperature remains nearly constant is expressed as[9,10]

Particle convective component:
$$h_{pc} = \frac{1}{R_w + 0.5R_{packet}} \quad (3)$$

where R_w is the thermal contact resistance at the wall and R_{packet} is the thermal resistance of packets of emulsion particles. When the tube is regularly "swept" by bubbles with a certain frequency (that is, blanketed by bubbles for a time fraction, f_B), the overall bed-to-surface heat transfer becomes

$$\bar{h}_{pc} = (1 - f_B)h_{pc} = \frac{(1 - f_B)}{R_w + 0.5R_{packet}} \quad (4)$$

Gelperin and Einstein[9] and Baskakov et al.[10] show that Eq. 4 is applicable to both large and small particles. This approach is in agreement with that of Grewal and Saxena,[11] who suggested that the bed-to-surface heat transfer is dependent on particle residence time at the tube surface and particle concentration near the surface. Shorter particle residence time and higher

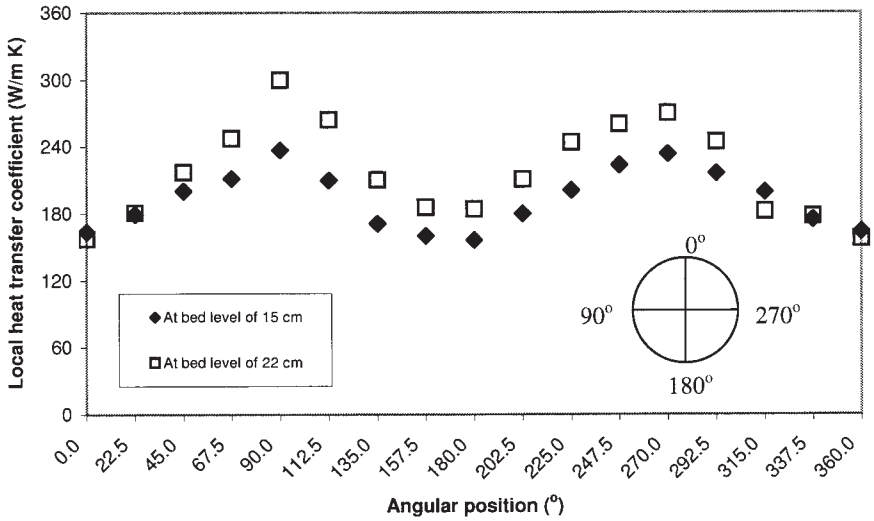

Figure 5. Variation in local heat-transfer coefficient over the tube surface with different probe position.

Cylindrical bed (ϕ 240 mm) with the presence of three vertically aligned horizontal tubes located at 50, 220, and 290 mm above the distributor; 0.6 mm sand; bed static height 350 mm.

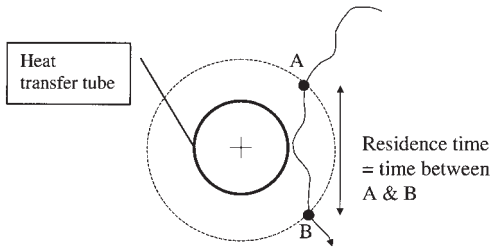

Figure 6. Residence time determination using particle trajectory.

dense phase fraction near the surface both contribute to higher values of local heat-transfer coefficient.[12] Parameters for Eqs. 2 and 4 are detailed in Table 1.

Experimental Conditions

Experiments were carried out first to establish heat-transfer coefficients for the material of interest and their variation with the position of the measurement on the heat-transfer surface and, second (using the noninvasive particle tracking technique, PEPT), to determine particle trajectories close to heat-transfer surfaces. Heat-transfer measurements were carried out in a cylindrical aluminum-walled bed of diameter 240 mm. The gas distributor was a drilled perforated aluminum plate with a mesh attaching to the underside. The plate was 1 cm thick and contained 80 holes of 2 mm diameter, arranged on a 20 mm^2 pitch. Sand, with a mean diameter of 0.6 mm and a particle density of 2600 kg/m^3 (u_{mf} = 0.27 m/s), was used as the bed material. According to Geldart's classification,[16] this has the characteristics of Group B.

All heat-transfer experiments took place using tubes of circular cross section, oriented with their axes horizontal. A heat-transfer probe was designed, as shown schematically in Figure 2. It is a cylindrical Bakelite™ rod with an outer diameter of 2 cm and length of 355 mm. Bakelite™ is used because of its good thermal and electrical insulation properties. Three slots, with dimensions of 6 × 0.6 × 0.2 cm (length × width × depth), were machined on the probe surface. Three strip heaters were then installed in these three surface slots. Each strip heater was prepared by winding 80 μm copper wire over the strip, the ends of which were brought out through an axial cylindrical channel. The strip heaters were arranged at a distance 1.5 cm apart from each other. Each heater could be activated independently. This design allows measurement of the heat-transfer coefficient not only at different angular positions (by rotating the entire assembly), but also in three different axial locations. Only the middle heater was used in the current study and its position was always close to the center of the bed. The supplied heat flux can be determined as

$$h = \frac{q}{S_{pr}(T_s - T_b)} \tag{10}$$

where q is the power supplied to the heater (W), S_{pr} is the surface area of the heater (m^2), T_s is the surface temperature of the heater (°C), and T_b is the bed temperature (°C). The power supply was set at 0.9 W for all heat-transfer experiments because this was found to give reliable and reproducible results.[6] The bed temperature was measured using a Type K thermocouple located at a distance of 22 cm above the distributor plate. Another Type K thermocouple was attached to the heater surface to measure its surface temperature. Both thermocouples were connected to a computer for data recording.

Results and Discussion

The presence of immersed tube(s) has a local effect on particle movement in fluidized beds, leading to different contact conditions at different angles around the tube and thus different local heat-transfer coefficients around the tube surface. Figure 3a shows the effects of angular position and superficial velocity on the local heat-transfer coefficient. Similar angular variations have been reported by others (for exam-

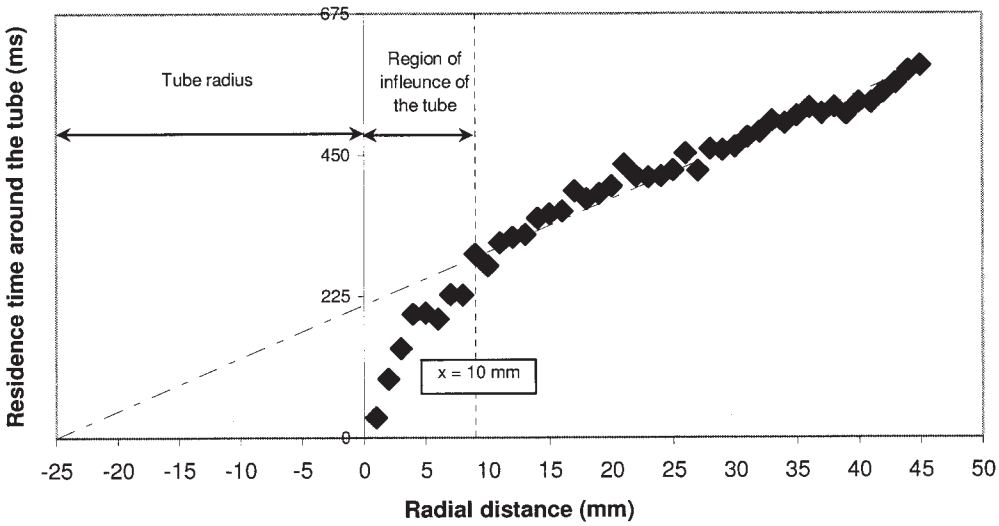

Figure 7. Variation in residence time around tube with increasing outer radius of the annulus around the tube.

Rectangular bed (0.6 × 0.06 × 1.5 m), 0.6 mm sand, bed static height 400 mm, and tube positioned at a bed level of 280 mm above the distributor.

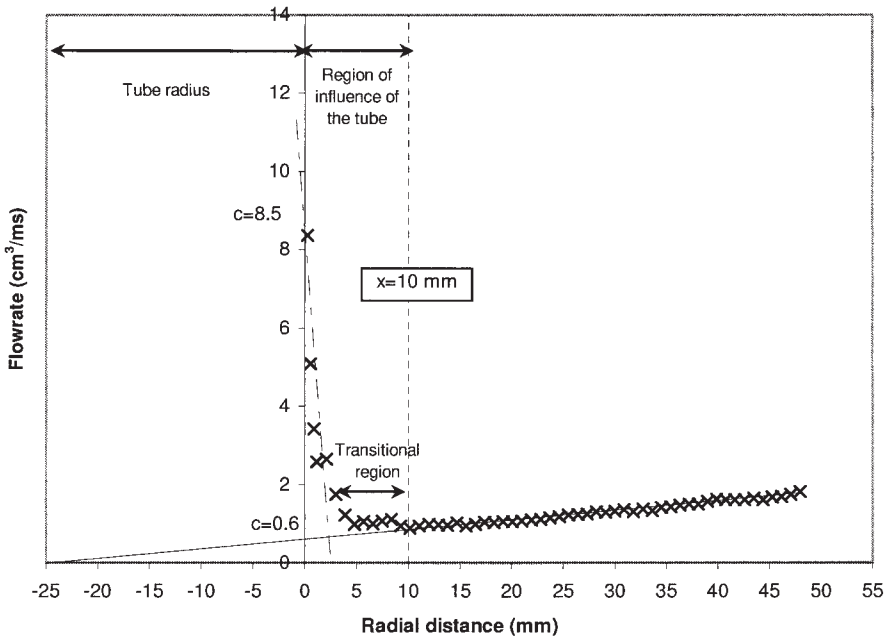

Figure 8. Variation in flow rate with increasing radial distance from the tube.

Rectangular bed (0.6 × 0.06 × 1.5 m), 0.6 mm sand, bed static height 400 mm, and tube positioned at a bed level of 280 mm above the distributor.

ple, Botterill[4]). At a superficial velocity slightly above the minimum fluidization velocity (u_{exe} = 0.08 m/s), maxima were found at the tube horizontal positions (that is, 90 and 270°; 0° is taken as vertically upward). Minima were found both directly upstream (vertically downward) and downstream (vertically upward), which correspond to the intermittent presence of an air film and the presence of a region of almost stagnant solids, respectively. Other evidence for the presence of the air film and a defluidized region in the upstream and downstream regions, respectively, can be found in the experimental studies of Glass and Harrison[17] and Sitnai and Whitehead[18] and in discrete element (DEM) computational studies by Wong[6] (see Figure 3b). A higher heat-transfer coefficient at the tube horizontal positions may be attributed to the vigorous particle motion in this region, resulting in more frequent replacement of solids.[9] This kind of angular variation in heat-transfer coefficient can be found typically at superficial velocity slightly higher than minimum fluidization velocity, u_{mf}.[7,9]

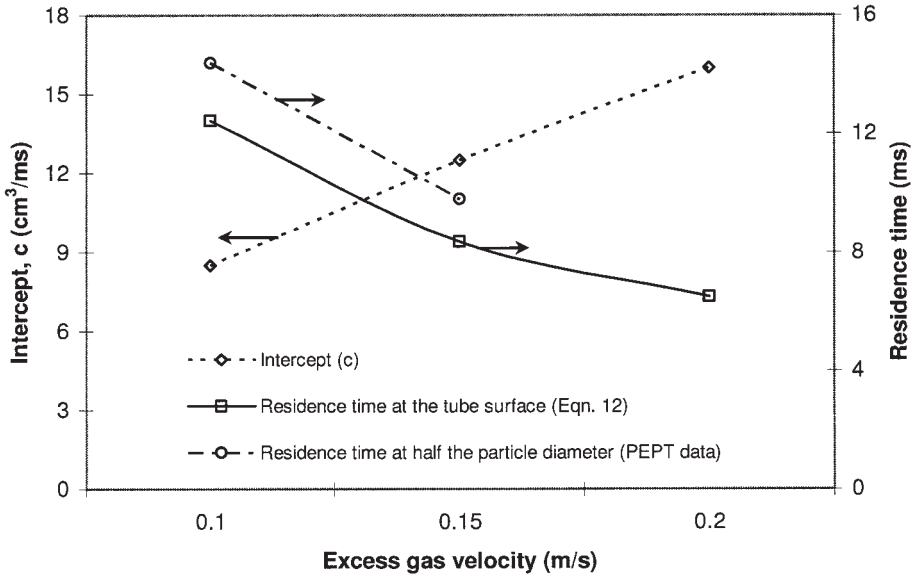

Figure 9. Dependency of intercept and residence time on the excess gas velocity.

Rectangular bed (0.6 × 0.06 × 1.5 m), 0.6 mm sand, bed static height 400 mm, and tube positioned at a bed level of 280 mm above the distributor.

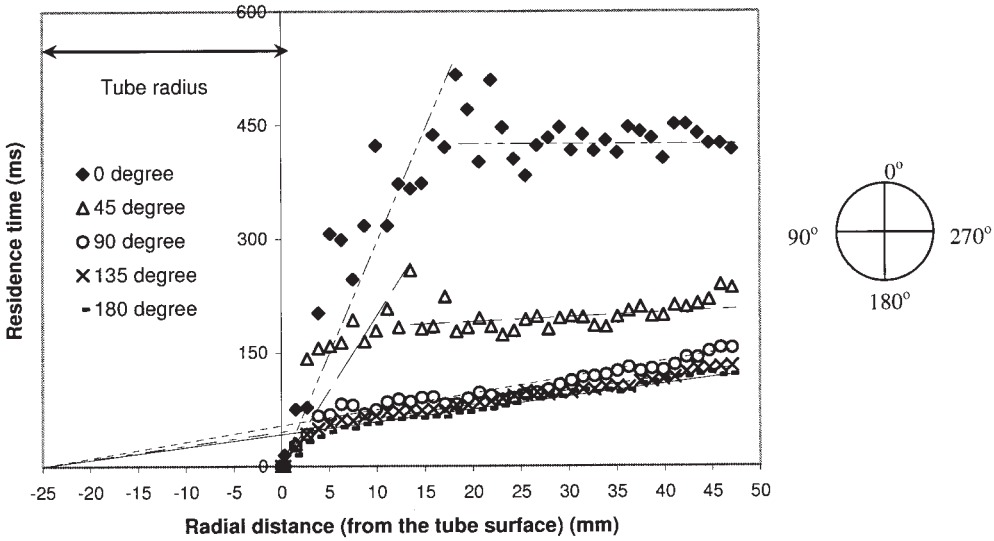

Figure 10. Dependency of residence time on the radial distance from the tube and tube angular position.

Rectangular bed (0.6 × 0.06 × 1.5 m), 0.6 mm sand, bed static height 400 mm, and tube positioned at a bed level of 280 mm above the distributor.

With an increase in excess gas velocity (that is, u_{exe} values from 0.08 to 0.50 m/s), the local heat-transfer coefficient increases overall, as the replacement of particles near the surface becomes more frequent. The positions of the maxima move from 90° (or 270°) to about 65° (or 295°). A further increase in excess gas velocity (that is, u_{exe} values from 0.50 to 0.80 m/s) leads to a decrease in the local heat-transfer coefficient at all angular positions. As mentioned earlier, an increase in heat-transfer coefficient with increasing superficial velocity can be attributed to the more frequent replacement of particles at the heat-transfer surface. However, a further increase in the gas flow will have an adverse effect because it causes the number of bubbles at the surface to increase and therefore reduces the opportunity for heat transfer because of the decline in average solids concentration.[9]

Figure 4 shows the effect of increasing superficial velocity on averaged heat-transfer coefficient over the tube circumference. As expected, the heat transfer increases with increasing gas velocity, to a maximum value, here at about $3u_{mf}$. This shape of curve is typical for Geldart's Group B particles, for which the particle convective component is most significant. The maximum heat-transfer coefficient can be predicted from the dimensional correlation proposed by Zadbrodsky[19]:

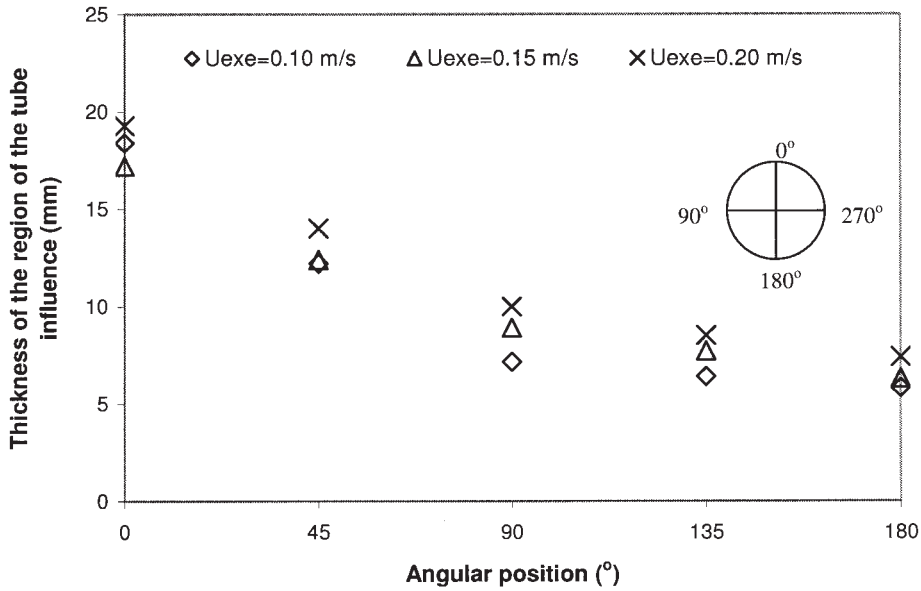

Figure 11. Variation in thickness of the region of influence of the tube with angular position and excess gas velocity.

Rectangular bed (0.6 × 0.06 × 1.5 m), 0.6 mm sand, bed static height 400 mm, and tube positioned at a bed level of 280 mm above the distributor.

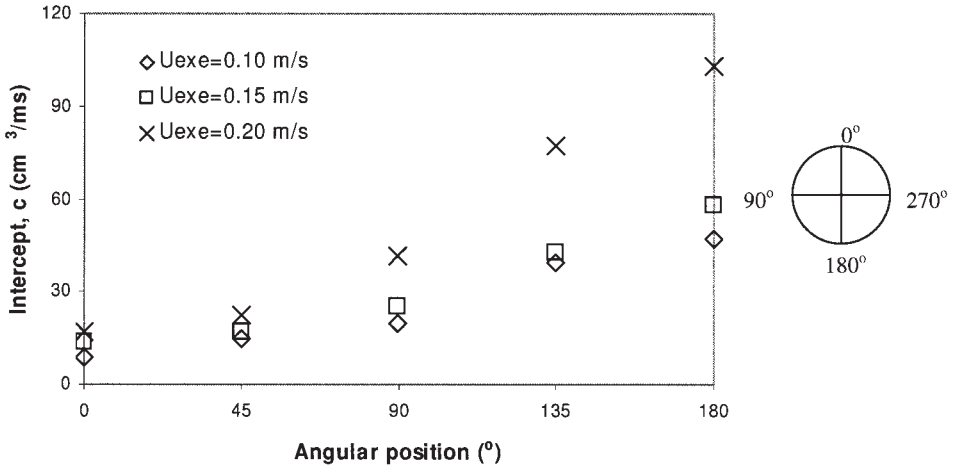

(a)

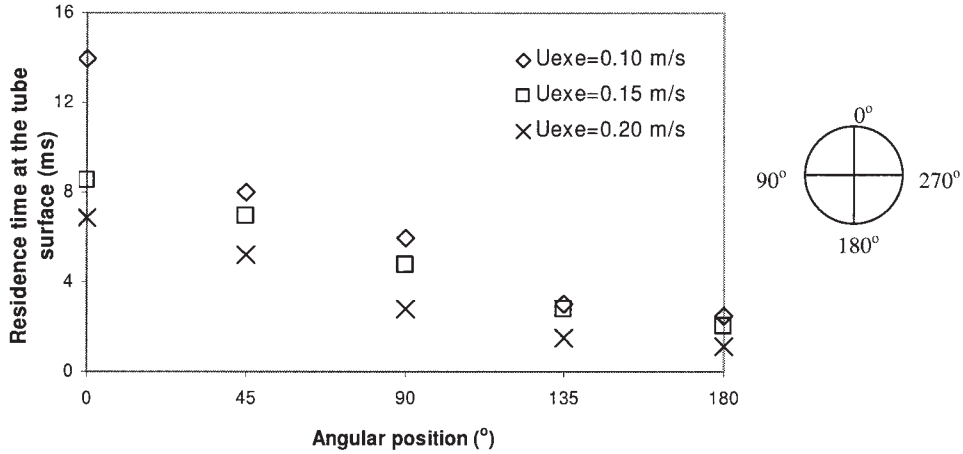

(b)

Figure 12. Effects of excess gas velocity and angular position on: (a) intercept, c; and (b) residence time at the tube surface.

Rectangular bed (0.6 × 0.06 × 1.5 m), 0.6 mm sand, bed static height 400 mm, and tube positioned at a bed level of 280 mm above the distributor.

$$h_{\max} = 35.8\rho_p^{0.2}k_g^{0.6}d_p^{-0.36} \tag{11}$$

This correlation is recommended for use only with Geldart's Group B particles.[4] With the appropriate properties of the particles of interest, the maximum (spatially averaged) heat-transfer coefficient is predicted to be 280 W m^{-2} K^{-1}, which is in good agreement with the data presented in Figure 4.

The effect of probe position on the bed-to-surface heat-transfer coefficient in a bed with three vertically aligned horizontal tubes at an excess gas velocity of 0.20 m/s is shown in Figure 5. Overall, it is clear that the local heat-transfer coefficient increases with increasing elevation of the tube within the bed: the average heat-transfer coefficient value increases from h_{ave} = 200 W m^{-2} K^{-1} at a bed level of 150 mm to h_{ave} = 220 W m^{-2} K^{-1} at a bed level of 220 mm. This trend is expected, given that bubbles in beds of particles of this size grow and rise faster at higher bed levels as a result of bubble interaction and coalescence, thereby increasing the particle replacement rate near the heat-transfer surface.

Interpretation of experimental results with PEPT data

The key element in the packet renewal theory developed by Mickley and Fairbanks[1] is the particle residence time at the heat-transfer surface. In the present study, residence time distribution results are used to interpret the experimental heat-transfer data. A single tracer particle—of the same material and mean size as those of the bulk—is inserted into the bed. Locational inaccuracy means that it is not possible to determine with certainty whether the tracer makes contact with the tube surface. Therefore the method shown schematically in Figure 6 was adopted: a notional cylindrical surface is drawn around the heat-transfer tube at a certain distance from it, and the time for

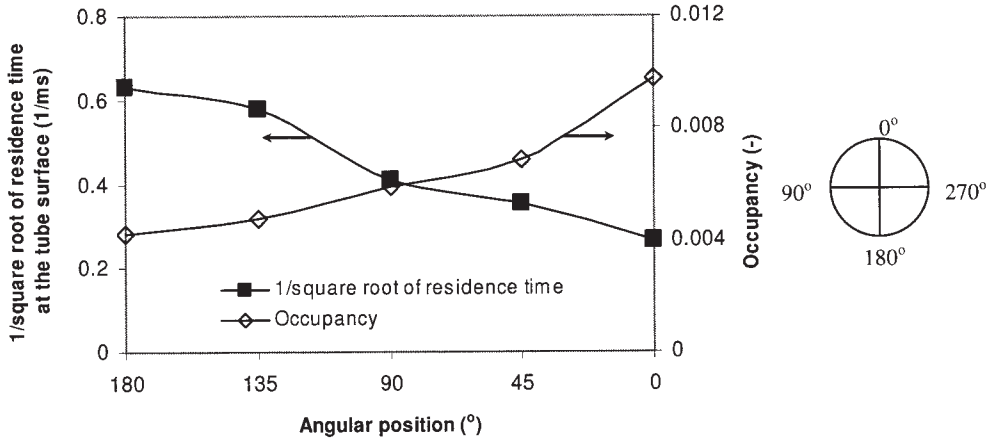

Figure 13. Distribution of the inverse of square root of residence time and occupancy at a distance of 10 mm away from the tube at an excess gas velocity of 0.10 m/s.

Rectangular bed (0.6 × 0.06 × 1.5 m), 0.6 mm sand, bed static height 400 mm, and tube positioned at a bed level of 280 mm.

which the tracer remains within the annular region around the tube is determined. Figure 7 shows the residence time in this annular region around a tube positioned at a bed level of 280 mm above the distributor, as a function of the outer radius of the annulus. For these experiments, the particles were unchanged but a rectangular bed was used, with dimensions of 0.6 × 1.5 × 0.06 m (width × height × depth). The bed was filled to a depth of 40 cm and was operated at ambient conditions with an operating velocity of 0.10 m/s and one horizontal immersed tube with a diameter of 5 cm (on the centerline). Particles were taken randomly from the bulk to be irradiated as tracers. The tracking time for each experiment was about 1.5 h.

With an increase in the thickness of the annulus within which the residence time is obtained, it can be seen that there is a change in the slope of the residence time plot. As the thickness of the annulus becomes large, compared with the radius of the tube, the presence of the tube becomes less significant and a linear relationship would be expected between residence time and annulus dimension, as observed here at larger annular dimensions. The slope of the plot after 10 mm can be extended back to the tube centerline. The point at which the measurements deviate from this line defines the "region of influence" of the tube. By carrying out a similar analysis for excess gas velocities of 0.15 and 0.20 m/s, the thickness of the region of influence of the tube for these two velocities was estimated at about 10 mm, independent of gas velocity. Wong[6] shows that the mean residence time within this region is inversely proportional to the square root of the excess gas velocity ($u - u_{mf}$), as suggested by Bock.[20]

The PEPT data on residence time in the annular region around the tube may be interpreted in terms of the volumetric flow rate, which is determined by dividing the volume of the annulus by the corresponding residence time. The annular volume was based on a tube radius of 25.3 mm (to allow for the particle radius) and radial distance. The result is plotted in Figure 8 as a function of the thickness of the annulus, for an excess gas velocity of 0.1 m/s. Similarly to Figure 7, the thickness of the region of influence of the tube is about 10 mm. The plot is linear for distances beyond this region of influence and the line can be extrapolated to the origin at the tube center. For distances $\lesssim$ 4 mm, the points can be extrapolated to give an intercept at the tube surface. This in turn allows the asymptotic residence time at the tube surface to be obtained; this residence time appears to be

$$\tau_0 = \frac{\pi R^2 z}{c} \tag{12}$$

where R is the tube radius, z is the tube thickness, and c is the intercept. Similar analysis was carried out for excess gas velocities of 0.15 and 0.20 m/s. The effect of excess gas velocity on both the intercept and the residence time at the tube surface is shown in Figure 9. When the excess gas velocity is increased, it is clear that the intercept is increased, and there is a corresponding decrease in the residence time at the tube surface, as expected. This residence time is consistent with values obtained directly from the PEPT residence time data at a distance from the tube of half the particle diameter. This intercept is an indicator of the hindrance caused by the tube to particles moving in its vicinity.

Figure 10 shows the variation in residence time around the tube surface with increasing thickness of the annulus for an excess gas velocity of 0.10 m/s. It is clear that the data obtained only at angular positions of 90, 135, and 180° can be extended back to the tube centerline. The presence of the tube has a more significant influence on particle motion in the upstream region than at other angular positions. As expected, Figure 11 shows that the thickness of the region of the tube's influence decreases with increasing angular position, giving an average value of about 10 mm, in agreement with previous findings. By plotting the volumetric flow rate in the vicinity of the tube as a function of the thickness of the annulus (as described previously), we can obtain the intercept values and the corresponding residence time at the tube surface for different angular positions and excess gas velocities. Figure 12 presents the intercept values and residence time distribution around a tube positioned at a bed level of 280 mm above the distributor in a rectangular bed with one immersed tube. The operating excess gas velocity was in the range 0.10–0.20 m/s. Longer residence time and lower

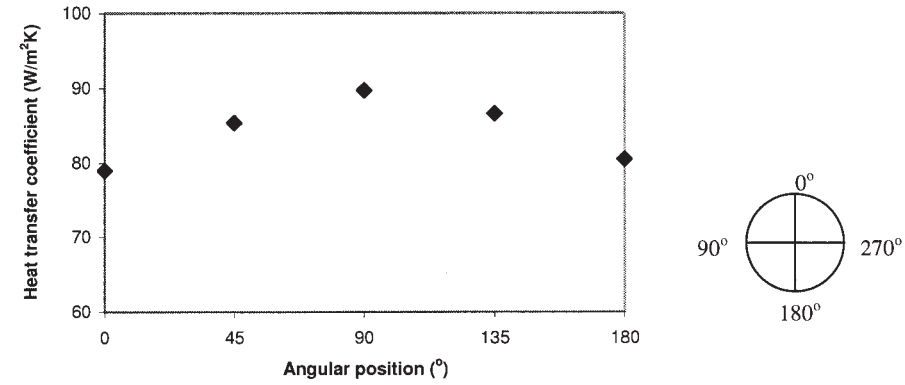

a)

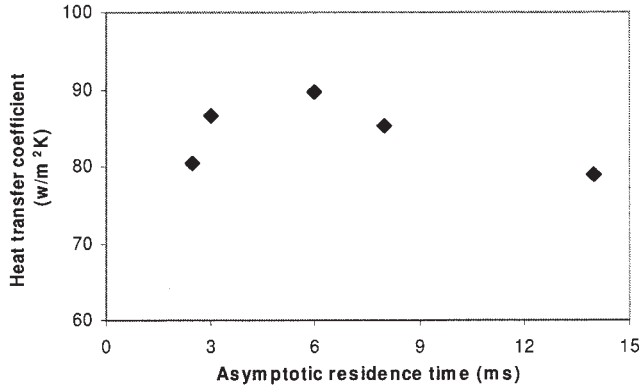

b)

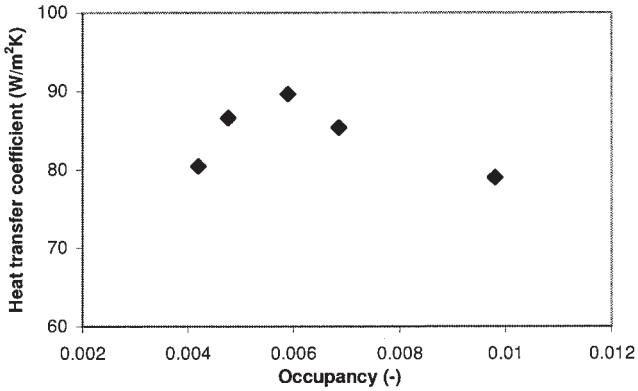

c)

Figure 14. (a) Test of Eq. 4; and variation of calculated heat-transfer coefficient with (b) asymptotic residence time and (c) occupancy.

Rectangular bed (0.6 × 0.06 × 1.5 m), 0.6 mm sand, bed static height 400 mm, and tube positioned at a bed level of 280 mm.

intercept values can be found in the downstream region, whereas a lower residence time and higher intercept values are observed in the upstream region.

Following Mickey and Fairbanks[1] and Gelperin and Einstein,[9] the overall particle convective component can be expressed as

$$\bar{h}_{pc} \propto \text{solids concentration} \times \frac{1}{\sqrt{\text{residence time, } \tau}} \qquad (13)$$

Shorter particle residence time (so that particles are frequently replaced) and higher average solids concentration will contrib-

ute to higher values of the local heat-transfer coefficient.[11,12] In this case, the local average solids concentration can be estimated from the "occupancy" * values derived from the PEPT measurements.

Figure 13 shows the distributions of the inverse of the square root of residence time at the tube surface and of tracer occupancy in a rectangular bed with one tube. The upstream region has a shorter residence time and a lower value of occupancy (that is, lower solids concentration), whereas the downstream region shows a higher value of residence time and higher occupancy. Both tracer residence time and occupancy values for the tube horizontal position (90°) are intermediate between those for upstream and downstream regions, which is in agreement with experiments by Kim et al.[12] It is these two factors that contribute to the existence of maximum values of local heat-transfer coefficient at the horizontal position, as indicated in Figure 14. The shape of Figure 14a is similar to those shown in Figures 3 and 5.

Conclusions

For an immersed tubular heat-transfer surface within a bubbling fluidized bed, the local heat-transfer coefficient varies with angular position around the tube surface. Maxima in the heat-transfer coefficient occur at or around the tube horizontal positions (that is, 90 and 270°), although the precise position varies with operating gas velocity. The heat-transfer coefficient is found to increase with increasing superficial gas velocity, but a further increase can result in lower heat-transfer coefficient as a result of the competing effects of increased particle replacement at the surface and decreasing local solids fraction. The heat-transfer coefficient is also observed to increase with increasing probe elevation above the gas distributor. Using positron emission particle tracking (PEPT), a method has been developed to determine the particle residence time in the vicinity of the heat-transfer surface. This yields a measure of the "region of influence" of the tube, which in this case is about 10 mm for a 5 cm diameter tube. The local heat-transfer coefficient is predicted from the local time-averaged solids fraction and the inverse of the square root of the particle residence time at the surface. Both these terms have been estimated from PEPT data and the result has been successfully used to explain the observed angular variation in heat-transfer coefficient. It is suggested that this method of particle tracking therefore captures the essential features of interest in predicting local heat-transfer coefficients.

Acknowledgments

The authors are grateful to the Committee of Vice-Chancellors and Principals (CVCP) for the award of an ORS (Overseas Research Studentship) scholarship to Y. S. Wong. The helpful comments of Dr. Don Glass from the University of Edinburgh are acknowledged with thanks. The reviewers are acknowledged for very helpful and insightful comments on the first manuscript.

Literature Cited

1. Mickley HS, Fairbanks DF. Mechanism of heat transfer of fluidised beds. *AIChE J.* 1955;1:374-384.
2. Parker DJ, Dijkstra AE, Martin TW, Seville JPK. Positron emission particle tracking studies of spherical particle motion in rotating drums. *Chem Eng Sci.* 1997;52:2011-2022.
3. Parker DJ, Broadbent CJ, Fowles P, Hawkesworth MR, McNeil P. Positron emission particle tracking—A technique for studying flow within engineering equipment. *Nucl Instrum Methods Phys Res.* 1993; A326:592-607.
4. Botterill JSM. Heat transfer to immersed surfaces in fluidised and packed fluidised beds. In: *Fluid Bed Heat Transfer.* London: Academic Press; 1975;Chapter 5:229-277.
5. Gloski D, Glicksman L, Decker N. Thermal resistance at a surface in contact with fluidised bed particles. *Int J Heat Mass Transfer.* 1984; 27:599-610.
6. Wong YS. *Experimental and Numerical Investigations of Fluidisation Behaviour with and without the Presence of Immersed Tubes.* PhD thesis. Birmingham, UK: University of Birmingham; 2003.
7. Botterill JSM. Fluid bed heat transfer. In: Geldart D, ed. *Gas Fluidization Technology.* Chicester, UK: John Wiley & Sons Ltd.; 1986; Chapter 9:219-258.
8. Ozkaynak TF, Chen JC. Emulsion phase residence time and its use in heat transfer models in fluidized beds. *AIChE J.*1980;26:544-550.
9. Gelperin NI, Einstein VG. Heat transfer in fluidised beds. In: Davidson JF, Harrison D, eds. *Fluidization.* New York: Academic Press; 1971; Chapter 10:471-540.
10. Baskakov AP, Berg BV, Vitt OK, Filippovsky NF, Kirakosyan VA, Goldobin JM, Maskaev VK. Heat transfer to objects immersed in fluidized beds. *Powder Technol.* 1973;8:273-282.
11. Grewal NS, Saxena SC. Maximum heat transfer coefficient between a horizontal tube and a gas–solid fluidised bed. *Ind Eng Chem Process Des Dev.* 1981;20:108-116.
12. Kim SW, Ahn JY, Kim SD, Lee DH. Heat transfer and bubble characteristics in a fluidised bed with immersed horizontal tube bundle. *Int J Heat Mass Transfer.* 2003;46:399-409.
13. Yagi S, Kunii D. Studies on effective thermal conductivities in packed beds. *AIChE J.* 1957;3:373-381.
14. Yagi S, Kunii D. Studies on heat transfer near wall surface in packed beds. *AIChE J.* 1960;6:97-104.
15. Botterill JSM, Denloye AOO. A theoretical model of heat transfer to a packed or quiescent fluidized bed. *Chem Eng Sci.* 1978;33:509-515.
16. Geldart D. Types of gas fluidization. *Powder Technol.* 1973;7:285-292.
17. Glass DH, Harrison D. Flow patterns near a solid obstacle in a fluidised bed. *Chem Eng Sci.* 1964;19:1001-1002.
18. Sitnai O, Whitehead AB. Immersed tubes and other internals. In: Davidson JF, Clift R, Harrison D, eds. *Fluidization.* Second Edition. New York: Academic Press; 1985;Chapter 14:473-493.
19. Zadbrodsky SS. *Hydrodynamics and Heat Transfer in Fluidized Beds.* Cambridge, MA: The MIT Press; 1966.
20. Bock HJ. Heat transfer in fluidized beds. Preprints of the 4th International Conference on Fluidization, Kashikojima, Japan; 1983:5.2.1-5.2.8.

* Occupancy is defined as the proportion of the total run time that the spacer spends within an individual volume element ("voxel") and, in a well-mixed system, is a surrogate for time-averaged density.

Manuscript received July 4, 2005, and revision received Aug. 21, 2006.